ELSEVIER

Journal of Molecular Catalysis A: Chemical 131 (1998) 243–257

JOURNAL OF MOLECULAR CATALYSIS A: CHEMICAL

Selected molecular surface structures determined by modern low-energy electron diffraction

M.A. Van Hove [a,*], G.A. Somorjai [a,b]

[a] *Materials Sciences Division, Lawrence Berkeley National Laboratory, Berkeley, CA 94720, USA*
[b] *Department of Chemistry, University of California, Berkeley, CA 94720, USA*

Received 1 July 1997; accepted 11 August 1997

Abstract

This article surveys a series of structural results obtained for the adsorption of small molecules (from CO to benzene) on the closest-packed metal surfaces by low-energy electron diffraction (LEED). Most of these results were obtained by detailed fitting of many structural parameters, primarily with automated tensor LEED. We discuss mainly qualitative aspects: adsorption sites, adsorbate orientation, molecular distortions and adsorbate-induced relaxations. Cases of special interest include: CO and NO monolayers adsorbed on metal surfaces, which require a revision of adsorption site assignments based on vibrational frequencies; various coadsorption structures exhibiting site changes due to the electron donor vs. acceptor character of the coadsorbates; intact di-σ ethylene adsorbed in a disordered and asymmetrical manner on Pt(111); intact acetylene on MgO(100), the first molecular and also first physisorbed adsorption structure determined in detail on an oxide surface; and the surface of an ultra-thin ice film, exhibiting unusually large vibration amplitudes of the outermost molecules.

Keywords: Low-energy electron diffraction; Adsorption site; Adsorbate orientation; Molecular distortion

1. Introduction

Brian Bent, to whose memory this article is dedicated, was deeply involved in many early structural studies of molecular adsorption on metal surfaces, in particular with the application of high-resolution electron energy loss spectroscopy (HREELS). Such work was extremely helpful in performing the more detailed crystallographic analyses of molecular adsorption by low-energy electron diffraction (LEED), both by eliminating many a priori possible structures and also by providing starting structures for crystallographic refinement.

In subsequent years, thanks to careful work like Brian's, a series of molecular adsorption structures was solved. This paper shows how far the field of surface crystallography with LEED, assisted by HREELS, infrared spectroscopy and other techniques, has progressed since Brian turned his attention to other topics, by discussing a series of structures of particular interest. This includes structures that were refined with more modern methods (primarily automated tensor LEED) or that needed to be revis-

* Corresponding author. Mailstop 66-200, Materials Sciences Division, Lawrence Berkeley National Laboratory, Berkeley, CA 94720, USA. Tel.: +1-510-486-6160; fax: +1-510-486-4995; e-mail: vanhove@lbl.gov

1381-1169/98/$19.00
PII S1381-1169(97)00269-0

ited (due to incorrect earlier assumptions in vibrational site assignments). We also present more complex molecular structures, made accessible by the maturation of earlier methods: this encompasses lower-symmetry structures, coadsorption structures and disordered structures.

We focus our attention here on small molecules, up to benzene in size, adsorbed or coadsorbed on two very similar types of close-packed metal surfaces, namely fcc(111) and hcp(0001). These are the systems that have been studied most in the last two decades. This discussion will concentrate on qualitative features like adsorption sites, orientations of adsorbed molecules and, to a lesser extent, adsorbate and substrate relaxations due to the adsorption process. More quantitative details can be found in the Surface Structure Database [1,2] and, for Ru(0001), in a very recent review article by Menzel [3]. It should be stressed that one or two techniques other than LEED (mainly forms of photoelectron diffraction) have been used to determine the details of a relatively small number of molecular structures; this paper will not address those structures.

In Sections 2–10, we address each selected type of molecule individually. We will then summarize and discuss observed trends across molecules in Section 11.

2. CO and NO monolayers on metal surfaces

The structure of adsorbed CO and NO monolayers is of current importance because the site assignments based on measured CO and NO vibrational stretch frequencies appear to be misleading in a number of cases. The latest case concerns a 3/4 fractional monolayer of CO on Rh(111): following recent core electron spectroscopy experiments, the original site assignment has had to be revised, as confirmed by LEED. We first discuss this case, followed by other CO and NO molecular layers on several fcc(111) and hcp(0001) metal surfaces. We will also review structural information known for the coadsorption of CO or NO with other molecular or atomic adsorbates.

The adsorption of CO on Rh(111) was investigated in 1980 by HREELS [4], up to the saturation coverage of 3/4 fractional monolayer, which orders into the Rh(111) + (2 × 2)-3CO structure (the index 3 indicates that three CO molecules fit within each (2 × 2) unit cell). The C–O stretch frequencies for this high-coverage system were measured to be 2070 and 1870 cm^{-1}: based on these frequencies and packing considerations, this structure was originally thought to consist of CO molecules in both top and bridge sites. A simple site assignment based on C–O stretch frequencies relates the single-coordinated top site to frequencies above about 2000 cm^{-1}; the twofold coordinated bridge site is assigned to frequencies in the approximate range 1850–2000 cm^{-1}; and the threefold coordinated hollow sites are assigned to frequencies below about 1850 cm^{-1} (there are two such sites, fcc-hollow and hcp-hollow, which are not distinguished in this respect) [5]. It now appears that this assignment has been taken too strictly by many surface scientists, including in the early study of the high-coverage structure of CO on Rh(111).

For Rh(111) + (2 × 2)-3CO, the 2070 cm^{-1} frequency thus lies in the range customarily assigned to top-site adsorption, while the 1870 cm^{-1} frequency lies just above the boundary between the ranges customarily assigned to bridge- and hollow-site adsorption. Focusing on a frequency comparison with rhodium-containing metal-carbonyl clusters, a clear preference for bridge-site adsorption was derived. Similarly, the lower-coverage (1/3 monolayer) Rh(111) + ($\sqrt{3} \times \sqrt{3}$)R30°-CO system has a C–O stretch frequency of 2000 cm^{-1}, which was assigned to top sites [4].

These site assignments were confirmed by early LEED analyses for both structures [6–8]. The first LEED analysis of Rh(111) + (2 × 2)-3CO started from the top + bridge site assignment and found reasonable agreement between

theory and experiment, if one allowed the top-site CO molecules to shift sideways by about 0.5 Å to 'near-top' sites in the direction of the nearest hollow sites [7,8]; such a shift is quite plausible in order to relieve the excessive CO–CO compression implied by direct on-top adsorption. The early LEED analysis did not consider the top/hollow site combination, guided by HREELS and the apparent success with the top/bridge site combination, but also because of the associated computational expense which was large in those days. However, later attempts at refining this structure with automated tensor LEED led to physically unreasonable atomic positions (A. Barbieri, unpublished data), primarily in the form of excessive substrate relaxations in the second metal layer, relative to prior experience: we now know that this behavior in LEED often implies that something is incorrect in the assumed structural model.

More recently, core electron spectroscopy experiments were interpreted to be incompatible with the HREELS site assignment at high coverage, and suggested an alternative model consisting of CO molecules in three sites: top, fcc hollow and hcp hollow [9]. Now, a detailed reanalysis of the LEED data has confirmed this new model, illustrated in Fig. 1, by producing a significantly better fit of theory to experiment [10]. By contrast, a LEED reanalysis of the low-coverage Rh(111) + ($\sqrt{3} \times \sqrt{3}$)R30°-CO structure [10] confirms both the initial vibrational assignment of top sites and its subsequent LEED structure determination [6], while refining it further. In addition, the core electron spectroscopy experiments are also consistent with top-site adsorption at low coverages [9].

The new site assignment for the high-coverage system links the 2070 cm^{-1} C–O stretch frequency with a top site and the 1870 cm^{-1} frequency with both types of hollow site. The low-coverage 2000 cm^{-1} frequency remains linked to a top site. There thus appears to be a significant up-shift of the hollow-site C–O stretch frequency in this system, relative to metal carbonyl clusters, from whose structures the

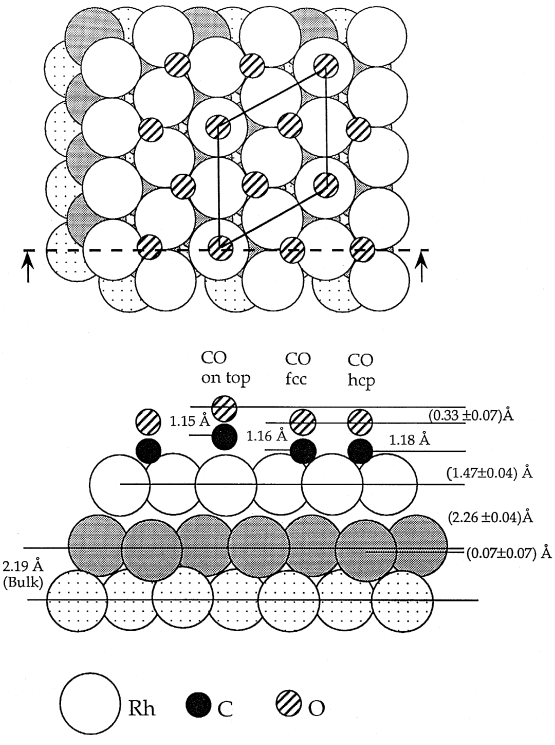

Fig. 1. New geometry for Rh(111)+(2×2)-3CO, in top view (at top) and side view (at bottom). Selected interlayer spacings are indicated.

standard frequency-site assignment rules were derived [11]. This may be due to lateral dipole coupling [12] or chemical interactions [13] between the CO molecules, which are both very probable effects in the high-density CO layer.

Similar, sometimes more dramatic inconsistencies have emerged in recent years for several other cases of CO or NO adsorption on fcc(111) metal surfaces. For CO, the standard C–O stretch frequency assignment in the system Ni(111) + c(4 × 2)-2CO would imply bridge site bonding. However, a LEED analysis finds hollow-site bonding, in both fcc and hcp hollow sites [14] (the index 2 in the structure notation indicates that two CO molecules fit within the c(4 × 2) unit cell). For CO, it thus appears that the discrepancies occur only for high-coverage structures, in which chemical interactions between crowded CO molecules are most likely to increase the C–O stretch frequencies.

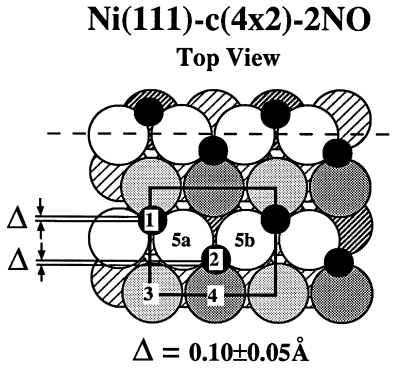

Fig. 2. Top view of the Ni(111)+c(4×2)-2NO structure. A c(4×2) unit cell is outlined. The distance Δ indicates a lateral shift of the molecules by about 0.1 Å from the hollow sites towards top sites, due to intermolecular repulsion: this repulsion also induces a possible slight tilt of these molecules from the surface normal by $4\pm4°$ away from each other, as illustrated in Fig. 3. The dashed line shows a pseudoglide plane, ignoring deeper metal layers.

Compared to CO overlayers, NO overlayers have been studied much less frequently, especially with detailed structural analyses. The corresponding assignment rule linking the adsorption site to the N–O stretch frequency is even less reliable, in part because there are relatively few cluster compounds on which to base such site assignments. Furthermore, the possible structural complexity in inorganic nitrosyl compounds is much greater than that found in metal carbonyl complexes. Judging from the poor applicability of such an assignment rule for the case of CO, it might be argued that one should not even attempt to derive one for NO adsorption. In fact, vibrational assignment predicts sites of lower coordination than are found by structural determination for at least two systems: Ni(111) + c(4 × 2)-2NO, in which LEED finds occupation of both fcc and hcp hollow sites [15,16], cf. Figs. 2 and 3, very much like the corresponding CO adsorption structure described above, and Pt(111) + (2 × 2)-NO [15], in which LEED finds occupation of fcc hollow sites.

It is interesting to note that NO produces a high-coverage structure on Rh(111) that is very similar to the high-coverage CO structure discussed above: Rh(111) + (2 × 2)-3NO; this structure was analyzed in moderate detail by a nonautomated LEED search [17]. The vibrational frequencies and the similarity in coverage and periodicity to the corresponding CO structure suggest also a similarity in adsorption sites: as a result, coadsorption in top and hollow sites was not investigated by LEED analysis. The best resulting structure was then indeed essentially identical to the old result for Rh(111) + (2 × 2)-3CO: one NO molecule in bridge site and two NO molecules in near-top sites in each unit cell. With the revision of the high-coverage CO structure described above, the corresponding high-coverage NO structure is however also put into question. Recently, in fact, independent evidence from X-ray photoelectron diffraction has suggested that NO occupies top sites and both kinds of hollow sites [18]. It would therefore not be surprising if a new LEED analysis

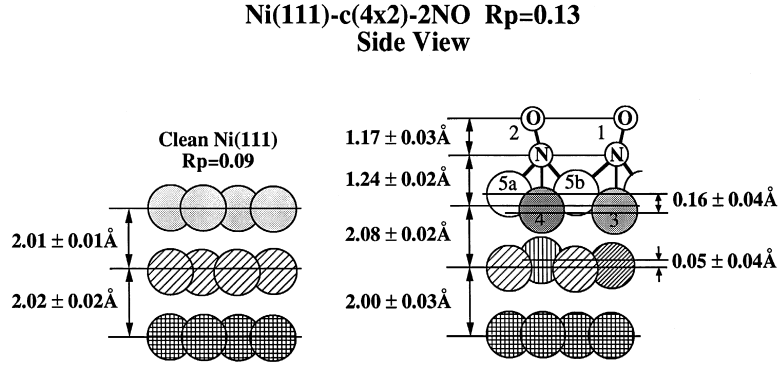

Fig. 3. Side view of the Ni(111) + c(4 × 2)-2NO structure shown in Fig. 2, together with the clean Ni(111) surface for comparison.

of the Rh(111) + (2 × 2)-3NO system would confirm the top/hollows arrangement which now seems much more likely. Such a conclusion would once more confirm the danger of using vibrational frequencies to identify adsorption sites of molecules like CO and NO.

Coadsorption of CO or NO with other atoms or molecules has been studied in detail for a number of structures. It is well known (e.g., from vibrational frequency shifts) that coadsorbates that donate electrons favor a displacement of CO and NO toward higher-coordination adsorption sites, especially hollow sites. Examples involving atomic coadsorption are the pair of structures Ru(0001) + (2 × 2)-Cs + CO and Ru(0001) + (2 × 2)-Cs + 2CO [19] (the notation implies that each (2 × 2) unit cell contains one Cs atom and one vs. two CO molecules): the latter structure has twice as much CO as the former, with the additional CO occupying fcc hollow sites, while the initial CO occupies hcp hollow sites in both structures; by contrast, in the absence of Cs, CO occupies top sites on this surface.

Coadsorption of CO with other molecules is exemplified by two related structures for benzene, Rh(111) + (3 × 3)-C_6H_6 + 2CO and Pd(111) + (3 × 3)-C_6H_6 + 2CO [20]: here, CO occupies hollow sites, hcp on Rh and fcc on Pd; by comparison, in the absence of benzene, CO would occupy top sites on Rh(111), but the same fcc hollow sites on Pd(111), however, at intermediate coverages, pure CO on Pd(111) occupies bridge sites. Thus, benzene acts as an electron donor, a fact well-known from work function change measurements. NO coadsorbed with benzene on Ru(0001), in the structure Ru(0001) + (3 × 3)-C_6H_6 + 2NO, yields hcp hollow sites for NO [21]. Finally, coadsorption of CO or NO with ethylidyne (C_2H_3) on Rh(111) also yields hollow sites, since ethylidyne acts as an electron donor [22]. However, it is not the same hollow in the two cases: CO selects the hcp hollow site in Rh(111) + c(4 × 2)-CO + C_2H_3, but NO selects the fcc hollow site in Rh(111) + c(4 × 2)-NO + C_2H_3.

Different behavior is found in coadsorption with electron acceptors. Thus, oxygen coadsorption maintains the top site for CO in both Ru(0001) + (2 × 2)-O + CO [23] and Ru(0001) + (2 × 2)-2O + CO [24], unchanged from the pure CO overlayer. The same holds for Rh(111) + (2 × 2)-O + CO, while for Rh(111) + (2 × 2)-O + 2CO the additional CO can only occupy hcp hollow sites, for steric reasons (the O atoms and initial CO molecules occupy fcc hollow and top sites, respectively) [25]: in fact, these hcp hollow sites are so unfavorable that the experiment could only occupy 60% of them with CO.

A note is in order about the orientation of CO and NO molecules relative to the surface. In most of the cases described above, the average orientation of the CO molecules is perpendicular to the surface. However, in several instances, a more detailed analysis has shown that the CO axis is in fact tilted by about 8–20° [10,26,27]: this is generally interpreted to represent a non-static wagging motion of the molecule, due to thermal vibrations. The distinction between static and dynamic thermal tilt is not easy to establish; a temperature-dependent analysis would be needed to clarify this. A few of the CO and NO structures described in this section do exhibit some static tilting: Ni(111) + c(4 × 2)-2CO and Ni(111) + c(4 × 2)-2NO (cf. Fig. 3) show very small tilts of the molecules, which is allowed by the overall lowered surface symmetry in the rectangular c(4 × 2) unit cell and is probably taking place to relieve crowding; Ru(0001) + (2 × 2)-2O + CO shows a static tilt by 17° from the surface normal, which breaks the overall surface symmetry and may be due to the incipient formation of CO_2.

3. N_2 monolayers on Ru(0001)

N_2 is isoelectronic to CO and can thus be expected to show similarities with CO. This has been confirmed by LEED for the case of adsorption on Ru(0001), as well as for coadsorption with oxygen on the same substrate. Pure N_2

yields the structure Ru(0001) + ($\sqrt{3} \times \sqrt{3}$)R30°-N_2 with intact molecules standing perpendicular and unbent at top sites [28], just like CO on Ru(0001). This result is not changed by coadsorption with oxygen in the structure Ru(0001) + (2 × 2)-O + N_2 [29]; in this case no evidence for a static tilt is found, in contrast to the corresponding CO structure.

4. Ethylene monolayers on Pt(111)

A disordered layer of ethylene was analyzed by LEED on Pt(111) at 200 K at a saturation coverage of about 1/4 fractional monolayer [30]. It is disordered at any temperature, producing a diffuse LEED pattern below the 250 K transition to ethylidene and then ordered ethylidyne. Below 250 K the molecules are intact, according to a variety of other techniques. The LEED study is the first detailed structural analysis of intact adsorbed ethylene and confirms the expectation of 'di-σ' bonding, but in an asymmetrical manner. However, this result is controversial, because it is counterintuitive, and the uncertainties on structural parameters are relatively large, because of a relatively small experimental database (despite the use of diffuse intensity vs. energy curves, as opposed to single-energy diffraction patterns); also, the occupation of two inequivalent sites gives many parameters that must be fit, further enlarging error bars.

The relatively large error bars and consequently lowered reliability of this structure analysis should be viewed as follows. Some structures (like also the ice surface discussed in Section 10), are inherently harder to analyze than others. One major reason, especially in these examples, is the practical difficulty of obtaining a large and reliable enough experimental data set of LEED intensities. This may be due to the inherent weakness of diffuse intensities (as in the ethylene case), or to a delicate or dynamic surface (both of these apply to the ice case). Therefore, the LEED result becomes relatively less informative than in the surfaces which are 'better behaved'. Nevertheless, LEED can deliver information not available from other techniques. For instance, with ethylene on Pt(111), our LEED analysis gives a larger error bar (see below) than a NEXAFS study of the C–C bond length does, but NEXAFS provides no information at all about the position of the molecules with respect to LEED. Thus, the LEED result remains of considerable utility in providing information, supplementing that available from other techniques. As usual in controversial cases, studies with other techniques are called for to verify the LEED results.

The diffuse LEED analysis finds occupation of both types of hollow sites, cf. Fig. 4. Nevertheless, if one ignores the second metal layer, the two adsorption geometries are identical within error bars: only the second metal layer distinguishes these two sites. In both sites, the

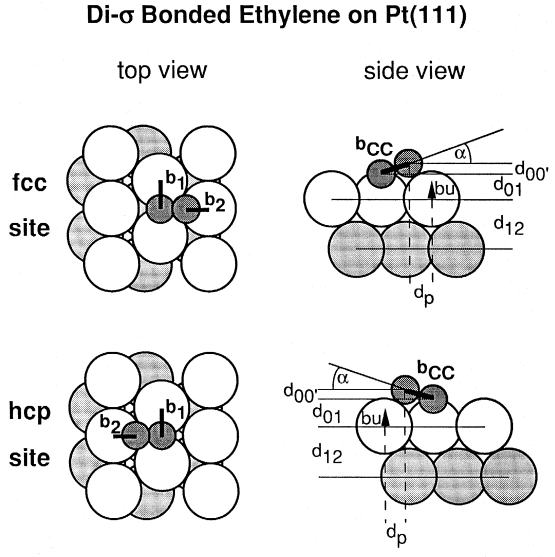

	α	b_1	b_2	b_{CC}	bu	d_p	$d_{00'}$	d_{01}	d_{12}
fcc site	23° $^{+21°}_{-11°}$	1.92 Å ±0.15 Å	2.07 Å ±0.30 Å	1.56 Å ±0.50 Å	0.03 Å ±0.07 Å	0.83 Å ±0.25 Å	0.61 Å ±0.07 Å	1.32 Å ±0.12 Å	2.27 Å ±0.05 Å
hcp site	22° $^{+21°}_{-11°}$	1.96 Å ±0.15 Å	2.05 Å ±0.30 Å	1.53 Å ±0.40 Å	0.02 Å ±0.07 Å	0.74 Å ±0.25 Å	0.57 Å ±0.07 Å	1.35 Å ±0.12 Å	2.27 Å ±0.05 Å

Fig. 4. Adsorption geometry of disordered C_2H_4 on Pt(111), occupying both fcc-hollow sites (top diagrams) and hcp-hollow sites (bottom diagrams). Top and side views are given at left and right, respectively. As detailed in the table, the local geometries in both sites are indistinguishable (H is omitted).

molecular C–C axis is tilted by $22^{+21\circ}_{-11}$ from the surface plane, with one C atom in a bridge site and the other C atom towards a top site. The tilt allows the Pt–C distances to be reasonable for both C atoms: 1.94 ± 0.15 Å at the bridge-bonded site vs. 2.06 ± 0.15 Å at the near-top-bonded site, after averaging between both hollow sites. The C–C distance is particularly uncertain, 1.55 ± 0.45 Å (UPS [31] and NEXAFS [32,33] found 1.49 and 1.50 Å, respectively), and hydrogen positions could not be determined. More interesting is that the substrate shows only small relaxations, such as a 0.025 ± 0.07 Å buckling of the top Pt layer, suggesting a relatively weak bonding to the molecule; larger buckling on the scale of 0.07–0.20 Å is often induced by more strongly adsorbed species like CO, ethylidyne and especially atoms.

The asymmetrical bonding of ethylene, with inequivalent C positions, comes as a surprise: however, no symmetrical site gave a satisfactory fit between LEED theory and experiment. The asymmetrical sites are in fact consistent with infrared spectroscopy measurements [34], in which the C–C stretch could be detected, possibly indicating a tilted C–C axis (on the other hand, the authors of the infrared study did propose consistency with a nontilted species, by invoking electron motion perpendicular to the surface during vibration parallel to the surface).

5. Ethylidyne monolayers on Pt and Rh(111)

Ethylidyne forms a very stable adsorbed species on several metal surfaces; it is a chemical dead end in the decomposition of ethylene. Its adsorption structure was determined long ago by LEED in the two systems Pt(111) + (2 × 2)-C_2H_3 [35] and Rh(111) + (2 × 2)-C_2H_3 [36]. These two structures were refined more recently by automated tensor LEED [37], confirming the earlier results, but still not determining hydrogen positions, cf. Figs. 5 and 6. The CCH_3 species are oriented on average perpendicularly to the surface, but exhibit (presumably thermal) tilts by 7° at 90 K on Pt and 11° at 240 K on Rh, relative to the surface normal. Also

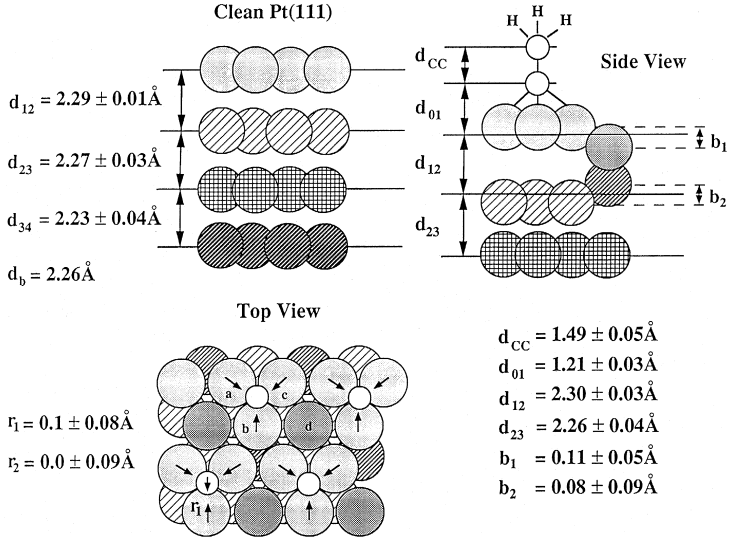

Fig. 5. Top right and bottom left: side and top views of Pt(111) + (2 × 2)-C_2H_3 (H omitted). The molecule is assumed for this illustration to be nontilted (i.e., fit assuming the full threefold rotational and mirror symmetry of the substrate). Shading distinguishes buckled atoms in each layer; the buckling is exaggerated for clarity. The interlayer spacings d_{ij} involving metal layers are measured between average atomic positions within the layers ($1/4$ of the buckling amount b_i from the triplets of coplanar metal atoms). Lateral metal displacements are labeled r_i for layer i. For comparison, the clean Pt(111) surface structure is shown at top left.

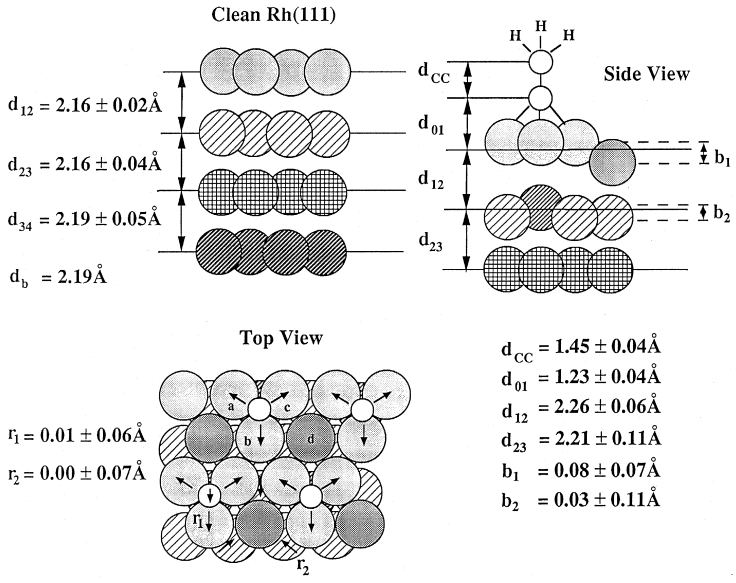

Fig. 6. Same as Fig. 5 for Rh(111) + (2 × 2)-C_2H_3 and clean Rh(111).

confirmed is a surprising difference in adsorption sites in these two systems: fcc hollows on Pt(111), but hcp hollows on Rh(111). The newer results also detected substantial relaxations in the substrate, similar to those induced by CO adsorption on such metal surfaces.

Ethylidyne was also studied by LEED when coadsorbed with either CO or NO on Rh(111), as mentioned above [22]. Intriguing is the result that CO addition displaces the ethylidyne from hcp to fcc hollow sites, while NO leaves the ethylidyne in hcp hollow sites. These structures should be submitted to a more refined structural determination with automated tensor LEED, in particular to explore possible static molecular tilts (which are in principle plausible due to the lower symmetry and the resulting asymmetrical molecule–molecule interactions in these structures), as well as any induced substrate relaxations.

6. Acetonitrile monolayers on Ni(111)

An interesting adsorption structure of lower symmetry is offered by the case of acetonitrile (CH_3CN) adsorbed in an ordered fashion on Ni(111): Ni(111) + (2 × 2)-CH_3CN, studied by automated tensor LEED [38] and illustrated in Fig. 7. Adsorption models had been proposed earlier on the basis of HREELS, XPS and NEXAFS data, which strongly suggested that the C–N bond axis lies nearly parallel to the surface, and that the C–N bond is of double-bond character. The LEED analysis allowed these conclusions to be verified, and to additionally determine the adsorption site as well as bond lengths and angles (except again for the hydrogen).

The C–N bond was indeed found to be tilted by only about 5° from the surface plane (the uncertainty on this number being larger than the value itself). The N atom lies approximately over an fcc hollow site, while the adjacent C atom lies closer to a nearest hcp hollow site, so that the C–N bond lies across a bridge site of the substrate. However, the C–C bond is tilted away from the surface plane by about 60° (forming a CCN bond angle of 123 ± 15°); this should be compared with the gas-phase molecule in which the CCN bond angle is 180°, i.e., CH_3CN is linear (except for the hydrogens of

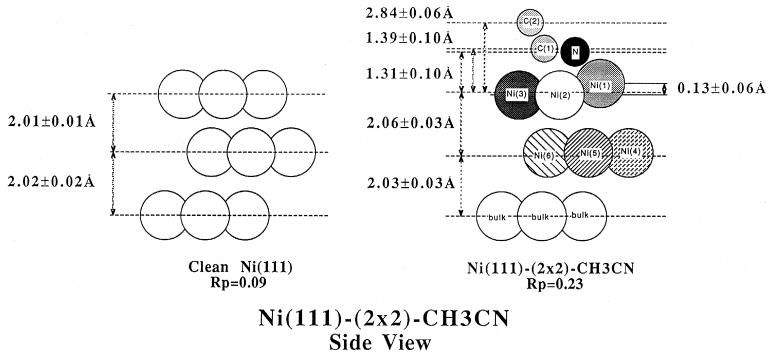

Fig. 7. At right, top and side views of Ni(111) + (2 × 2)-CH_3CN (H omitted). Selected interlayer spacings are shown (between averaged Ni planes where these are buckled as shown). Symmetrically inequivalent Ni atoms are shaded differently. Clean Ni(111) is shown at bottom left for comparison.

the methyl group). The CH_3C fragment can be viewed as an ethylidyne attached to the N atom, and its geometry appears to be very similar to the ethylidyne layers described above (apart from the permanent tilt in acetonitrile). The C–N and C–C bond lengths are rather uncertain, 1.28 ± 0.15 Å and 1.67 ± 0.15 Å, respectively, but point toward elongation of these two bonds by about 0.1 Å with respect to the gas-phase molecules, as is often found in adsorption.

7. Benzene monolayers on Ru(0001), Ni(111), Pd(111) and Rh(111)

The detailed adsorption structures of benzene has been studied on several metal surfaces, both as pure overlayers and coadsorbed with CO, NO or O. In all cases, the benzene molecules lie parallel to the surface (the H atoms may be bent upward from the surface, as predicted by total-energy calculations, but this could not be tested by LEED).

On Ni(111), a non-tensor LEED analysis including automated search was performed for the Ni(111) + ($\sqrt{7} \times \sqrt{7}$)R19.1°-C_6H_6 phase [39]. In this structure, each molecule covers three Ni atoms around an hcp hollow site, such that C–C bonds are parallel to the close-packed rows of metal atoms: thereby, a pair of C atoms caps one Ni atom. The C–C distances are lengthened to about 1.43 and 1.55 Å relative to the gas phase (where they all are 1.40 Å), thereby indicating a possible Kekulé-like distortion, while the C ring is essentially planar. Strong relaxations are observed in the substrate: metal atoms are 'pulled outward' by the C atoms to which they are directly bonded.

A structure that is very similar to the preceding one in terms of its superlattice, Ru(0001) + ($\sqrt{7} \times \sqrt{7}$)R19.1°-C_6H_6, nevertheless exhibits some interesting differences compared to the Ni(111) case [40]. First, on Ru(0001) each benzene is rotated by 30° about the surface normal, relative to its orientation on Ni(111), so that three of the C atoms are near top sites above three different Ru atoms surrounding an hcp hollow, while the other C atoms lie between the bridge sites linking those Ru atoms and fcc hollow sites beyond. As a result there are two types of C atoms between which there is a height difference of about 0.08 Å: the molecule is buckled into a crown-like shape (like the chair shape of cyclohexane). Nonetheless, the C–C bond lengths are essentially unchanged from the gas phase.

Staying with benzene on Ru(0001), but turning to coadsorption with electronegative O or NO, one finds two new structures [21]: Ru(0001) + (3 × 3)-C_6H_6 + 2O and Ru(0001) + (3 × 3)-C_6H_6 + 2NO. Here again, despite

identical superlattices, significant differences occur between the two. The addition of oxygen to the pure benzene layer does not markedly change the benzene location or its distortions from the gas phase. On the other hand, with NO the benzene is rotated by about 20° from the pure benzene case, thereby clearly breaking a mirror plane (while staying centered on the hcp hollow site), and a Kekulé-like distortion now becomes apparent (1.32 vs. 1.43 Å for alternating C–C bonds around the ring), at the same time as the buckling is reduced to perhaps 0.02 Å.

The coadsorption of benzene with CO on Rh(111) and Pd(111) in similar (3×3) structures had been studied much earlier, but without considering substrate relaxations [41,42]. Later refinements confirmed the results, giving more information and more confidence [43]. Both Rh(111) + (3×3)-C_6H_6 + 2CO (cf. Fig. 8) and

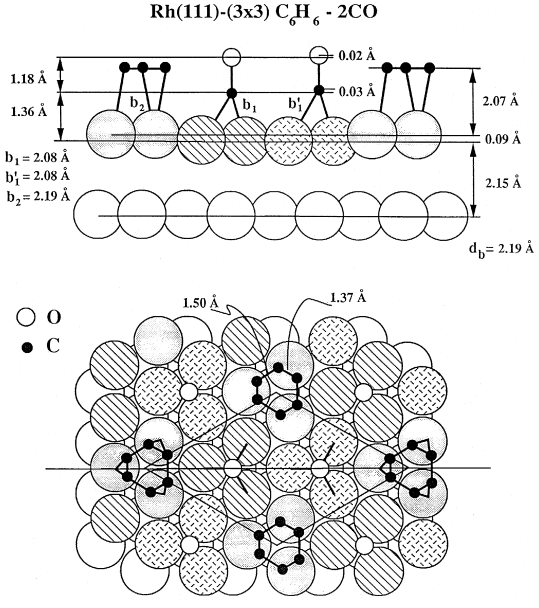

Fig. 8. Side view (upper panel) and top view (lower panel) of the best-fit symmetry-preserving Rh(111) + (3×3)-C_6H_6 + 2CO structure (H is omitted). Shading distinguishes symmetry-inequivalent atoms in the top metal layer; its buckling is exaggerated for clarity. The interlayer spacings involving metal layers are measured between buckled atomic positions within the layers, as indicated (d_b is the bulk metal value). Selected bonds are drawn and their lengths indicated.

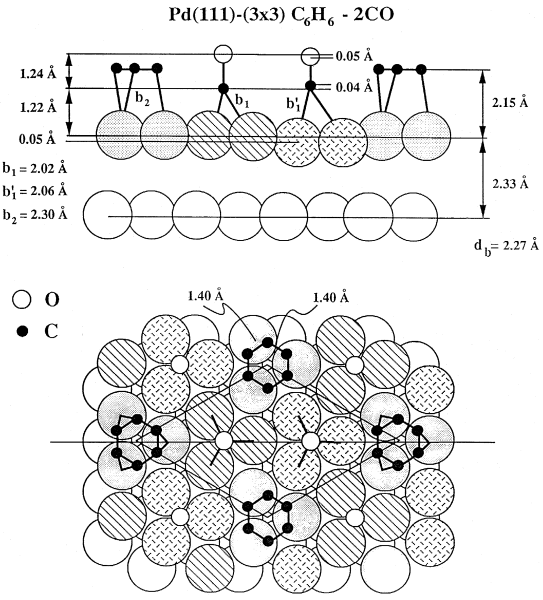

Fig. 9. Same as Fig. 8 for Pd(111) – (3×3)-C_6H_6 + 2CO.

Pd(111) + (3×3)-C_6H_6 + 2CO (cf. Fig. 9) exhibit occupation of hollow sites by all adsorbates; however, on Rh it is the hcp hollow sites and on Pd the fcc hollow sites that are selected (the reason for this difference is not understood, but it is consistent with the case of ethylidyne adsorbed on Rh(111) vs. Pt(111), cf. Section 5). A sizable Kekulé-like distortion is found on Rh (C–C distances alternating between 1.37 and 1.50 Å) but no such distortion is detected on Pd (C–C distances of 1.40 Å). Also, a larger substrate relaxation is observed on Rh than on Pd.

8. Acetylene monolayers on MgO(100)

We next describe a system with very weak molecular adsorption, namely the physisorption of acetylene (C_2H_2) on MgO(100). This case represents the first detailed structure analysis of molecular physisorption, and the first such analysis of adsorption on an oxide substrate [44].

At 90 K, acetylene adsorbs intact on MgO(100) in a (2×2) periodic arrangement. On MgO powders, earlier neutron diffraction

results indicated a herringbone arrangement within the (2×2) cell, implied by two glide planes perpendicular to the surface [45], but these could not determine the location of the molecules with respect to the substrate atoms. The LEED pattern on the single-crystal surface is consistent with the symmetry observed by neutron diffraction.

Before conducting a LEED analysis, semi-empirical potential calculations were applied to this surface, using rigid molecules and a rigid substrate [44]: these predicted flat-lying molecules, centered over Mg ions, at a relatively large height of about 2.50 Å above the oxide surface plane. Next, a detailed LEED analysis confirmed these predictions [44], which are consistent with weak bonding between molecule and oxide: no significant distortion was observed in either the substrate or the overlayer. The resulting structure of this MgO(100) $+ (2 \times 2)$-$2C_2H_2$ system is shown in Fig. 10.

While the adsorption energy is weak in this system, the semi-empirical potential calculations indicate the importance of electrostatic interactions in orienting and positioning the molecules. In particular, quadrupolar interactions dominate in this instance.

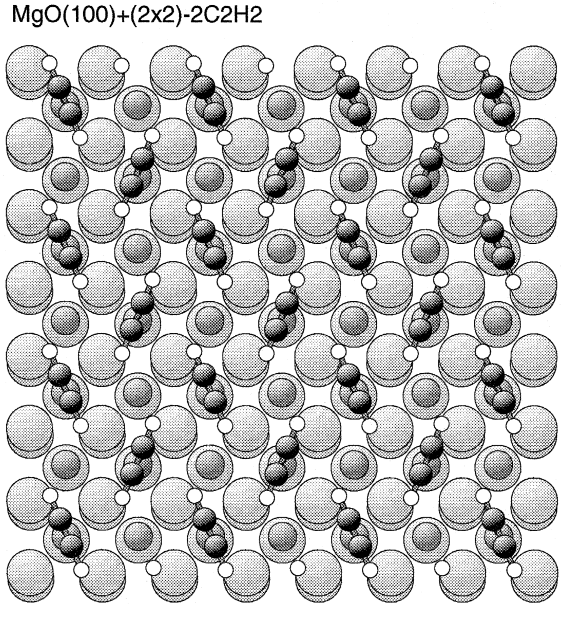

Fig. 10. Slightly off-normal view of MgO(100) + (2×2)-$2C_2H_2$, exhibiting flat-lying acetylene molecules centered over Mg ions (H assumed as in linear gas-phase acetylene). The molecular axes are oriented about 20° from the diagonal directions. Each substrate layer contains equal amounts of coplanar Mg and O ions.

9. Ice bilayers on Ru(0001)

Ice can produce a good lattice match on only a few metal surfaces and under certain conditions. On Ru(0001), this occurs for one bilayer, and only with D_2O rather than H_2O, forming a $(\sqrt{3} \times \sqrt{3})R30°$ structure. Thicker films do not order well on Ru, while a nondeuterated H_2O bilayer produces an incommensurate structure.

A bilayer is a basic building block of the stable, natural variety Ih of ice, which is held together by hydrogen bonds (each oxygen is bonded to another oxygen through one H atom between them). But the bilayer analyzed by LEED on Ru(0001) is very much flattened [46] compared to bulk ice Ih: the O–O interlayer spacing within the bilayer on Ru, rather than having the bulk value of 0.92 Å, is reduced almost tenfold to about 0.1 Å. This permits the oxygens of the outermost half-bilayer to approach closely to the metal surface and bond directly to metal atoms. In fact, the adsorption geometry is such that all oxygen atoms in this structure are at top sites above single Ru atoms. The oxygen atoms closest to Ru atoms induce larger local substrate relaxations than do the oxygens that are slightly more removed. The hydrogen atoms, once again, could not be located; this is in part due to the inherent disorder present in the hydrogen arrangement in any ice structure, and thus not only to the weakness of electron-hydrogen scattering.

10. Ice multilayers on Pt(111)

Contrary to the case on Ru(0001), it is difficult to produce an ordered bilayer structure of ice on Pt(111), whereas an ordered thicker film can be produced. Here we discuss such a molec-

ular film which was grown to a thickness of perhaps 10–20 Å; under these conditions LEED becomes insensitive to the substrate. Thus, we have a multilayer of ice, Ih-H_2O(0001), grown on Pt(111), and studied by automated tensor LEED at 90 K [47,48]. The LEED pattern is consistent with an unreconstructed (1×1) surface of bulk ice of type I (as opposed to the higher-pressure types II, III, etc). It could either be the naturally occurring hexagonal phase (Ih) or the metastable cubic phase (Ic): the LEED analysis favors the hexagonal variety, while the lateral lattice constant appears to be slightly expanded relative to the bulk of ice (perhaps to better approach the Pt lattice constant, with which there is an incommensurate relationship).

Surprising at first was the finding from LEED that the bulk ice lattice appears to be terminated between adjacent layers of a bulk bilayer (which we call 'half-bilayer termination', see Fig. 11), rather than terminated between two bilayers (called 'full-bilayer termination', see also Fig. 11) [47,48]. This was surprising because the full-bilayer termination would be expected to provide energetic stabilization due to the presence of more hydrogen bonds per (1×1) unit cell, compared with the half-bilayer termination. A solution, still to be proven experimentally, but which satisfies both LEED and total-energy considerations, is to assume that the external half bilayer of the outermost full bilayer actually vibrates so much as to be undetectable by LEED (due to a strong Debye–Waller factor), while still contributing the energetic stabilization of the additional hydrogen bonds. Thus, in LEED, the full-bilayer termination would appear indistinguishable from the half-bilayer termination. Such a model was confirmed to be reasonable by total-energy calculations and molecular-dynamics calculations [47,48], and is our hypothesis for the structure of this surface at 90 K. In particular, molecular dynamics predict rms vibrations of the outermost molecules to be of the order of 0.25 Å, which is compatible with the invisibility of those molecules to LEED, as verified by calculation [47,48].

The situation is now that we have no experimental proof of the presence of the water molecules in the external half bilayer of the outermost full bilayer: we only have strong theoretical evidence for the need to include them, and LEED calculations that show compatibility of this model with experiment. Thus, other experiments will be needed to provide the experimental proof of the existence of the strongly-vibrating outermost molecules. Recently, Glebov et al. [49] have studied this surface with atom scattering and detected an unusually 'soft' ice surface that has low-frequency vibrations and anomalously weak force constants: this is at least consistent with our hypothesis.

It is interesting that the molecular-dynamics calculations suggest that, with increasing temperature, the ice surface becomes gradually amorphous (above perhaps 140 K) and then

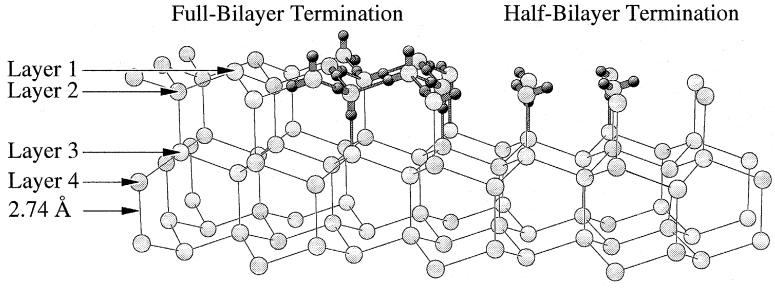

Fig. 11. Perspective side view of two terminations of natural (Ih) ice: the full-bilayer termination at left, which is believed to be the actual surface structure at 90 K, with large vibrations in layer 1, and the less credible half-bilayer termination at right (which is obtained by eliminating layer 1). H atoms (small circles) are only shown in some H_2O molecules as examples; otherwise only O atoms are shown, linked by H bonds.

even liquid-like at temperatures well below the bulk melting point of ice (above about 230 K) [50], consistent with experiment. The impression one gets of the ice surface is a highly dynamic one, with an unusual degree of vibration at the lowest temperatures, followed by hydrogen-bond breaking at slightly higher temperatures, and then surface melting well below the bulk melting point. This dynamic character may explain the catalytic role of ice in the creation of the Antarctic ozone hole [50,51] and may be the reason why ice is so slippery [51].

11. Summary and discussion

We have presented a series of cases of molecular adsorption on metal surfaces for which detailed structures have been obtained with LEED. They present special interest from different points of view: violation of standard CO site assignments based on vibration frequencies; adsorption site competition in coadsorption; distortions in the adsorbed molecule due to the adsorption; adsorbate-induced relaxations in the substrate; first detailed structural determinations of the weak chemisorption of intact ethylene on a metal surface, Pt(111), and of the physisorption of acetylene on MgO(100); large vibration amplitudes of the outermost water molecules in an ultra-thin film of ice grown on Pt(111).

Some general trends can be extracted from these various results.

Concerning adsorption sites, a trend emerges that is also known for atomic adsorbates [52]: with few exceptions, whenever adsorption occurs at hollow sites of fcc(111) or hcp(0001) substrates, the choice is the fcc hollow site on fcc(111) and the hcp hollow site on hcp(0001), as if to continue the bulk structure into the overlayer. This trend is also well known for atomic adsorbates. The main exceptions to this trend are: on Rh(111), donor adsorbates (C_2H_3, C_6H_6, as well as Na atoms [53]) prefer the hcp hollow site; however, CO coadsorbed with C_2H_3 on Rh(111) can take the hcp sites and displace the C_2H_3 to fcc sites; at higher coverages and with coadsorption, other sites may additionally be occupied, e.g., CO and NO can occupy both types of hollow sites simultaneously on Ni(111), while CO can occupy at the same time top, fcc-hollow and hcp-hollow sites on Rh(111); finally, benzene adopts the hcp site on Ni(111).

Other trends relate to relaxations induced by the adsorbates in the substrate; this trend holds not only for the molecular adsorbates discussed in this article, but also for atomic adsorbates [52]. Not surprisingly, weak adsorption (like that of intact ethylene on Pt and acetylene on MgO) induces no detectable relaxations in the substrate, or indeed in the adsorbate itself. A rather general rule appears to be that a strongly-bonded adsorbate will ‘pull out’ the substrate atoms to which it bonds, by about 0.1 Å. Substrate atoms that are bonded to more than one adsorbate are usually pulled out more than those bonded to only one adsorbate. This results in buckling of the outermost metal layer. Buckling effects are also found in the second metal layer, but they are harder to characterize in general terms. There are in addition lateral displacements (parallel to the surface) of substrate atoms near adsorbates: sometimes metal atoms are attracted toward an adsorbate site, while in other cases they are repelled away from that site; unfortunately, error bars on lateral relaxations are usually too large to take the results as definitive or to draw systematic conclusions.

An interesting attempt to examine the trends in adsorbate-induced relaxations for over 20 adsorption and coadsorption structures on Ru(0001) shows how difficult it is to extract systematic rules [3]. One simple trend seems to emerge, however, concerning the change of the average topmost interlayer spacing in the Ru: this spacing tends to increase with electronegative adsorbates (electron acceptors), while it tends to decrease with electropositive adsorbates (electron donors) or strongly polarizable adsorbates like Xe [17]. It appears that it will probably be necessary to take into account exactly

which substrate orbitals are modified by the bonding process, and in particular, which of these are bonding (and thus can shorten interatomic distances) and which are antibonding (and thus can lengthen interatomic distances).

As this brief review shows, a substantial database of results has now been established for the structure of adsorbed molecules on metal surfaces. But there is a clear need for many more results of similar or dissimilar type to allow generalizations to be made about the underlying mechanisms and their implications for catalysis and other surface processes. The variety of molecules that have not yet been submitted to structural determination at surfaces is staggering. This includes adsorption on stepped metallic surfaces, on other substrates (metallic alloys, semiconductors, other ionic compounds, etc.), and the surface of molecular solids (like the ice discussed here, which is the only such surface studied in detail up to now).

As a final point, there is also a need for more accurate results, especially concerning lateral interatomic distances (parallel to the surface), where current error bars are often too large to allow useful conclusions to be drawn. Higher accuracy depends on more reliable experimental angles of incidence, on larger measured data sets where possible, and on more attention to nonstructural parameters in the calculations (e.g., atomic scattering potentials, thermal vibrations and damping).

Acknowledgements

This work was supported in part by the Director, Office of Energy Research, Office of Basic Energy Sciences, Materials Sciences Division, of the U.S. Department of Energy under Contract No. DE-AC03-76SF00098. Fruitful collaborations are gratefully acknowledged with A. Barbieri, J.D. Batteas, J.-P. Bibérian, R. Döll, D. Ferry, D. Gardin, C.A. Gerken, M. Gierer, P.N.M. Hoang, G.-J. Kroes, N. Materer, C. Minot, U. Starke and J. Suzanne. Furthermore, J.N. Andersen, M. Gierer, D. Menzel and A. Wander are kindly thanked for providing results before publication.

References

[1] P.R. Watson, M.A. Van Hove, K. Hermann, NIST Surface Structure Database Ver. 2.0, NIST Standard Reference Data Program, Gaithersburg, MD, USA, 1996.
[2] P.R. Watson, M.A. Van Hove, K. Hermann, NIST Surface Structure Database Ver. 3.0, NIST Standard Reference Data Program, Gaithersburg, MD, USA, in preparation.
[3] D. Menzel, in: P. Soukiassian, G. Le Lay, M.A. Van Hove (Eds.), The Structure of Surfaces V, Surf. Rev. Lett., in press.
[4] L.H. Dubois, G.A. Somorjai, Surf. Sci. 91 (1980) 514.
[5] N. Sheppard, T.T. Nguyen, in: R.J.H. Clark, R.E. Hester (Eds.), Advances in Infrared and Raman Spectroscopy, Vol. 5, Heyden, London, 1978, p. 67.
[6] R.J. Koestner, M.A. Van Hove, G.A. Somorjai, Surf. Sci. 107 (1981) 439.
[7] M.A. Van Hove, R.J. Koestner, G.A. Somorjai, Phys. Rev. Lett. 50 (1983) 903.
[8] M.A. Van Hove, R.J. Koestner, J.C. Frost, G.A. Somorjai, Surf. Sci. 129 (1983) 482.
[9] A. Beutler, E. Lundgren, R. Nyholm, J.N. Andersen, B. Setlik, D. Heskett, Surf. Sci. 371 (1997) 381.
[10] M. Gierer, A. Barbieri, M.A. Van Hove, G.A. Somorjai, Surf. Sci. 391 (1997) 176.
[11] R.P. Eischens, W.A. Pliskin, Adv. Catal. 10 (1958) 1.
[12] J.P. Hollins, Surf. Sci. Rep. 16 (1992) 51.
[13] P. He, H. Dietrich, K. Jacobi, Surf. Sci. 345 (1996) 241.
[14] L.D. Mapledoram, M.P. Bessent, A. Wander, D.A. King, Chem. Phys. Lett. 228 (1994) 527.
[15] N. Materer, A. Barbieri, D. Gardin, U. Starke, J.D. Batteas, M.A. Van Hove, G.A. Somorjai, Surf. Sci. 303 (1994) 319.
[16] L.D. Mapledoram, A. Wander, D.A. King, Chem. Phys. Lett. 208 (1993) 409.
[17] C.T. Kao, G.S. Blackman, M.A. Van Hove, G.A. Somorjai, C.-M. Chan, Surf. Sci. 224 (1989) 77.
[18] Y.J. Kim, S. Thevuthasan, G.S. Herman, C.H.F. Peden, S.A. Chambers, D.N. Belton, H. Permana, Surf. Sci. 359 (1996) 269.
[19] H. Over, H. Bludau, R. Kose, G. Ertl, Surf. Sci. 331–333 (1995) 62.
[20] A. Barbieri, M.A. Van Hove, G.A. Somorjai, Surf. Sci. 306 (1994) 261.
[21] M. Stichler, R. Weimar, D. Menzel, Surf. Sci. 384 (1997) 179.
[22] G.S. Blackman, C.T. Kao, B.E. Bent, C.M. Mate, M.A. Van Hove, G.A. Somorjai, Surf. Sci. 207 (1988) 66.
[23] B. Narloch, G. Held, D. Menzel, Surf. Sci. 340 (1995) 159.
[24] B. Narloch, G. Held, D. Menzel, Surf. Sci. 317 (1994) 131.
[25] S. Schwegmann, H. Over, V. De Renzi, G. Ertl, Surf. Sci. 375 (1997) 91.
[26] H. Over, M. Gierer, H. Bludau, G. Ertl, Phys. Rev. B 52 (1995) 16812.

[27] M. Gierer, H. Bludau, H. Over, G. Ertl, Surf. Sci. 346 (1996) 64.
[28] H. Bludau, M. Gierer, H. Over, G. Ertl, Chem. Phys. Lett. 219 (1994) 452.
[29] H. Over, H. Bludau, R. Kose, G. Ertl, Chem. Phys. Lett. 243 (1995) 435.
[30] R. Döll, C.A. Gerken, M.A. Van Hove, G.A. Somorjai, Surf. Sci. 374 (1997) 151.
[31] T.E. Felter, W.H. Weinberg, Surf. Sci. 103 (1981) 265.
[32] J. Stöhr, J.L. Gland, J.A. Horsley, Chem. Phys. Lett. 105 (1984) 332.
[33] J. Stöhr, F. Sette, A.L. Johnson, Phys. Rev. Lett. 53 (1984) 1684.
[34] J. Fan, M. Trenary, Langmuir 10 (1994) 3649.
[35] L.L. Kesmodel, L.H. Dubois, G.A. Somorjai, J. Chem. Phys. 70 (1979) 2180.
[36] R.J. Koestner, M.A. Van Hove, G.A. Somorjai, Surf. Sci. 121 (1982) 321.
[37] A. Barbieri, M.A. Van Hove, G.A. Somorjai, in: X.D. Xie, S.Y. Tong, M.A. Van Hove (Eds.), The Structure of Surfaces IV, World Sci. (Singapore), 1994, p. 201.
[38] D.E. Gardin, A. Barbieri, J.D. Batteas, M.A. Van Hove, G.A. Somorjai, Surf. Sci. 304 (1994) 316.
[39] G. Held, M.P. Bessent, S. Titmuss, D.A. King, J. Chem. Phys. 105 (1996) 11305.
[40] C. Stellwag, G. Held, D. Menzel, Surf. Sci. 325 (1995) L379.
[41] R.F. Lin, G.S. Blackman, M.A. Van Hove, G.A. Somorjai, Acta Cryst. B 43 (1987) 368.
[42] H. Ohtani, M.A. Van Hove, G.A. Somorjai, J. Phys. Chem. 92 (1988) 3974.
[43] A. Barbieri, M.A. Van Hove, G.A. Somorjai, Surf. Sci. 306 (1994) 262.
[44] D. Ferry, P.N.M. Hoang, J. Suzanne, J.-P. Bibérian, M.A. Van Hove, Phys. Rev. Lett. 78 (1997) 4237.
[45] J.-P. Coulomb, Y. Lahrer, M. Trabelsi, I. Mirebeau, Mol. Phys. 81 (1994) 1259.
[46] G. Held, D. Menzel, Surf. Sci. 316 (1994) 92.
[47] N. Materer, U. Starke, A. Barbieri, M.A. Van Hove, G.A. Somorjai, G.-J. Kroes, C. Minot, J. Phys. Chem. 99 (1995) 6267.
[48] N. Materer, U. Starke, A. Barbieri, M.A. Van Hove, G.A. Somorjai, G.-J. Kroes, C. Minot, Surf. Sci. 381 (1997) 190.
[49] A. Glebov, A.P. Graham, A. Menzel, J.P. Toennies, J. Chem. Phys. 106 (1997) 9382.
[50] G.-J. Kroes, Surf. Sci. 275 (1992) 365.
[51] C. Seife, Science 274 (1996) 2012.
[52] U. Starke, M.A. Van Hove, G.A. Somorjai, Prog. Surf. Sci. 46 (1994) 305.
[53] M.A. Van Hove, Surf. Rev. Lett. 1 (1994) 9.